ISSN (Print) 1598-5385
ISSN (Online) 2233-6648
≪연구논문≫ Journal of the Korean Magnetics Society 35(6), 295-299 (2025) https://doi.org/10.4283/JKMS.2025.35.6.295

# Influence of Anisotropic Zeeman Energy on Néel-to-Bloch Transition in Chiral Domain Walls

**Ji-Sung Yu and Duck-Ho Kim***
*Center for Spintronics, Korea Institute of Science and Technology (KIST), Seoul 02792, Republic of Korea*

(Received 3 November 2025, Received in final form 22 November 2025, Accepted 25 November 2025)

**Chiral spin alignments are critical in modern magnetism, offering fundamental insights and prospects for spintronic applications. The stability of chiral domain walls (DWs) is governed by the interplay among DW anisotropy, Dzyaloshinskii-Moriya interaction (DMI), and Zeeman energies. While the influence of an external magnetic field applied along the DW normal is well established that of orthogonal in-plane field is less explored. Here, we theoretically uncover distinct Zeeman energy landscapes that govern the Néel-to-Bloch transition based on the external field orientation. For a magnetic field normal to the DW, the transition primarily depends on the DW anisotropy field. In contrast, when a field is applied along the DW plane, significantly large fields than the anisotropy and DMI-induced fields are required. This nonreciprocity arises from the competing influences of DMI and Zeeman interactions: in the field along the DW normal, DMI lowers DW energy alongside the Zeeman term, while in the field along the DW plane, it acts oppositely, increasing the DW energy. These findings reveal an unrecognized mechanism for field-direction-dependent DW chirality stabilization, offering new control strategies for chiral spin textures in magnetic nanostructures.**

**Keywords :** Chiral domain wall, Néel-to-Bloch transition, Dzyaloshinskii-Moriya interaction (DMI)

# 상이한 Zeeman 에너지에 의한 Néel에서 Bloch 자구벽 전환

**유지성 · 김덕호***
한국과학기술연구원 스핀융합연구단, 서울시 성북구 화랑로 14길5, 02792

(2025년 11월 3일 받음, 2025년 11월 22일 최종수정본 받음, 2025년 11월 25일 게재확정)

나선성 스핀 정렬은 현대 자기학 연구에서 중요한 현상으로, 근본적인 물리 이해와 함께 스핀트로닉스 응용의 가능성으로 많은 연구가 수행되어 왔다. 특히, 나선성 자구벽의 안정성은 자구벽 이방성, 드쟐로신스키–모리아 상호작용(Dzyaloshinskii-Moriya interaction, DMI), 그리고 외부 자기장에 의한 Zeeman 에너지 간의 상호작용에 의해 결정된다. 자구벽 법선 방향으로 외부 자기장이 가해질 때의 물리 현상은 잘 알려져 있지만, 자구벽에 수평한 방향의 자기장이 미치는 영향은 상대적으로 잘 연구되지 않았다. 본 연구에서는 자기장의 방향에 따라 Néel에서 Bloch 자구벽 전환이 서로 상이한 Zeeman 에너지 지형으로 변화함을 이론적으로 규명하였다. 자구벽 법선 방향으로 자기장이 가해지는 경우, Néel에서 Bloch 자구벽 전환는 주로 자구벽 이방성장에 의해 결정되지만, 자구벽 평면 방향으로 자기장이 가해지는 경우에는 자구벽 이방성과 DMI에 의해 유도되는 장보다 훨씬 큰 자기장이 필요함을 보였다. 이러한 비대칭성은 DMI와 Zeeman 상호작용의 경쟁적 역할에서 기인하며, 수직 방향 자기장에서는 두 항 모두 자구벽 에너지를 낮추는 반면, 수평 방향에서는 반대로 작용하여 DMI는 자구벽 에너지를 증가시킨다. 본 연구 결과는 자기장 방향에 따라 자구벽의 나선성이 안정화되는 새로운 물리 현상의 이해를 제시해, 자기 나노 구조 내 나선성 스핀 구조를 정밀하게 제어할 수 있는 새로운 가능성을 제안한다.

**주제어** : 나선성 자구벽, Néel에서 Bloch 자구벽 전환, 드쟐로신스키 모리아 상호작용


*Corresponding author: Tel: +82-2-958-5781, e-mail: uzes@kist.re.kr

## I. Introduction

Chiral spin alignments have gained considerable attention owing to their fundamental significance [1-5] and technological potential [6-11]. The creation of topological spin textures, such as Néel-type domain walls (DWs) [4,6-8,10-15] and magnetic skyrmions [1-3,5,9,10], and their efficient manipulation through spin- or orbital-current-induced torques are focal points in spintronics research [8,12,13,16-25]. The Dzyaloshinskii-Moriya interaction (DMI) is essential for stabilizing these chiral spin alignments [14,26-35] and for enhancing spin-orbit and orbital torques driving their current-induced motion [8,12,13,20]. Understanding these chiral spin phenomena relies on the magnetic DW energy, which comprises contributions from DW anisotropy, DMI, and Zeeman interactions.

Magnetic DWs generally adopt a Bloch-type configuration, to minimize the total wall energy, primarily determined by the demagnetizing field [14,31,34,36]. However, in systems exhibiting broken inversion symmetry and strong spin-orbit coupling, Néel-type DWs can stabilize, introducing a preferred orientation—or easy axis—of wall magnetization [14,26-35]. The energy difference between the easy and hard axes defines the anisotropy energy. The influence of a magnetic field applied along the DW normal (longitudinal geometry) on the DW energy is well established; in this configuration, the resulting energy difference corresponds to the DW anisotropy energy [31,37-39]. However, the influence of a magnetic field applied along the DW plane (orthogonal geometry) has been less studied.

Here, we theoretically reveal that this orthogonal geometry, the energy difference between the easy and hard axes no longer reflects the DW anisotropy energy. Unlike prior models focused on longitudinal field geometry, the orthogonal geometry provides a fresh perspective on the interplay between Zeeman and DMI contributions, uncovering hidden energy asymmetries within DWs.

## II. Result and Discussion

We first outline the theoretical framework proposed by Thiaville *et al*. to describe DW energy in systems with DMI [14,31]. In perpendicularly magnetized materials, sufficiently extended DWs adopt a Bloch-type configuration minimizing dipolar energy associated with in-wall magnetization. Fig. 1(a) illustrates the distinction between Néel- and Bloch-type DWs. The intrinsic energy difference arises from the DW anisotropy energy, while DMI introduces another competing energy. The interplay between DMI and DW anisotropy energies governs the equilibrium spin configuration within the wall, favoring either Néel- or Bloch-like states.

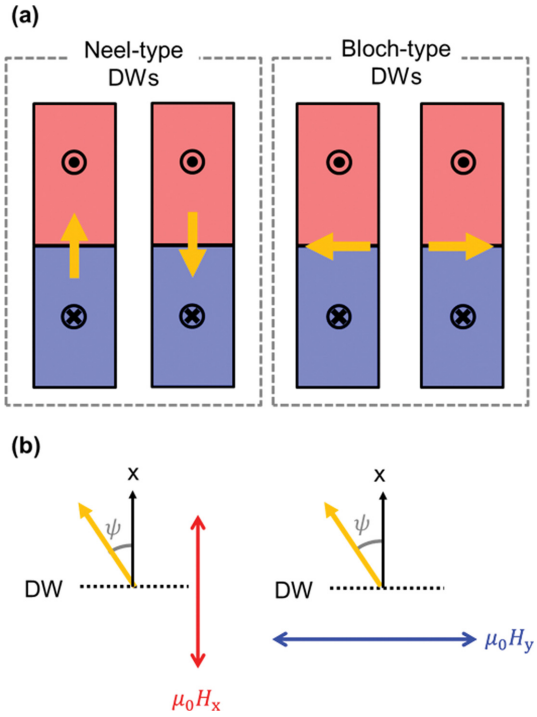


**Fig. 1.** (Color online) (a) Illustration of the distinction between Néel- and Bloch-type domain walls (DWs). The orange arrow indicates the magnetization at DW. (b) The response of the DW magnetization to an in-plane magnetic field for two representative cases: (1) field is applied along the DW normal (longitudinal geometry), and (2) field is applied along the DW plane (orthogonal geometry).

To examine the response of the DW magnetization to an in-plane magnetic field, we analyze two representative cases as shown in Fig. 1(b): (1) field is applied along the DW normal (longitudinal geometry), and (2) field is applied along the DW plane (orthogonal geometry). In the longitudinal geometry, for an initial Néel-type DW (where DMI energy exceeds DW anisotropy energy), Je *et al*. [31] demonstrated that the Zeeman energy required to rotate the DW magnetization to a Bloch configuration under a magnetic field along the x-axis equals the DW anisotropy energy.

Next, to analyze the orthogonal geometry, we apply an in-plane magnetic field along the y-axis $\mu_0 H_y$. The DW energy $\sigma_{DW}(\mu_0 H_y)$ can be expressed as

$$\sigma_{DW}(\mu_0 H_y) = \sigma_0 + \pi\lambda K_D \cos^2\psi - \pi\lambda M_S \mu_0 H_{DMI} \cos\psi - \pi\lambda M_S \mu_0 H_y \sin\psi, \quad (1)$$

where $\sigma_0$ is the energy density of a Bloch-type DW, $K_D$ is the DW anisotropy energy density, $\lambda$ is the DW width, $M_S$ is the saturation magnetization, and $\mu_0 H_{DMI}$ represents the

effective magnetic field induced by the DMI. The angle $\psi$ defines the azimuthal orientation of the magnetization within the DW, measured from the +x axis. Minimizing the DW energy with respect to $\psi$ (i.e., $\partial\sigma_{DW}/\partial\psi = 0$) yields

$$-2K_D\cos\psi_{eq}\sin\psi_{eq} + M_S\mu_0H_{DMI}\sin\psi_{eq} - M_S\mu_0H_y\cos\psi_{eq} = 0, \quad (2)$$

where $\psi_{eq}$ denotes the equilibrium magnetization angle. Because Eq. (2) is a quartic equation in $\cos\psi_{eq}$, obtaining an analytical solution is intractable. Therefore, $\psi_{eq}$ is calculated numerically for each applied field $\mu_0H_y$, enabling the monitoring of the evolution of $\sigma_{DW}$ as a function of $\mu_0H_y$.

In the examined system, a finite DMI stabilizes an initial Néel-type DW in the absence of an in-plane field ($\mu_0H_y$ = 0 mT). When $\mu_0H_y$ increases sufficiently to align the DW magnetization along the ±y direction, the wall gradually evolves into a Bloch-type configuration, corresponding to $\psi_{eq} = \pm\pi/2$. Fig. 2(a) presents the equilibrium angle $\psi_{eq}$ as a function of $\mu_0H_y$, calculated for $\sigma_0$ = 30 mJ/m$^2$, $\mu_0H_S$ = 30 mT, $\lambda$ = 1 nm, $M_S$ = 1 MA/m, and $\mu_0H_{DMI}$ = 50 mT [31,38,40], where the DW anisotropy field $\mu_0H_S$ is defined by the relation $K_D = M_S\mu_0H_S/2$.

At $\mu_0H_y$ = 0 mT, the DW exhibits a Néel-type orientation ($\psi_{eq}$ = 0). However, a sufficiently large $\mu_0H_y$ drives $\psi_{eq} \rightarrow \pm\pi/2$, signifying a Bloch-type wall. Interestingly, even when $\mu_0H_y$ reaches ±30 mT (red dashed lines) or ±50 mT (green dashed lines), corresponding to $\mu_0H_S$ and $\mu_0H_{DMI}$, respectively, $\psi_{eq}$ remains significantly below full alignment at $\pm\pi/2$ (inset of Fig. 2(a)). Even when $\mu_0H_y$ exceeds 200 mT, well above $\mu_0H_S$ and $\mu_0H_{DMI}$, the equilibrium DW angle $\psi_{eq}$ remains below $\pm\pi/2$. Extending the field range reveals that $\psi_{eq}$ reaches $\pm\pi/2$ only at $\mu_0H_y \cong 5.712$ T, nearly two orders of magnitude larger than $\mu_0H_S$ and $\mu_0H_{DMI}$, underscoring the strong field required to achieve full Bloch-type configuration. We denote this critical field as $\mu_0H_y^*$ (orange arrow in Fig. 2(a)).

To elucidate the origin of $\mu_0H_y^*$ relative to $\mu_0H_S$ and $\mu_0H_{DMI}$, we examined the evolution of $\sigma_{DW}$ as a function of $\mu_0H_y$ (Fig. 2(b)). As $\mu_0H_y$ increases, $\sigma_{DW}$ decreases monotonically, following the trend of the Zeeman energy

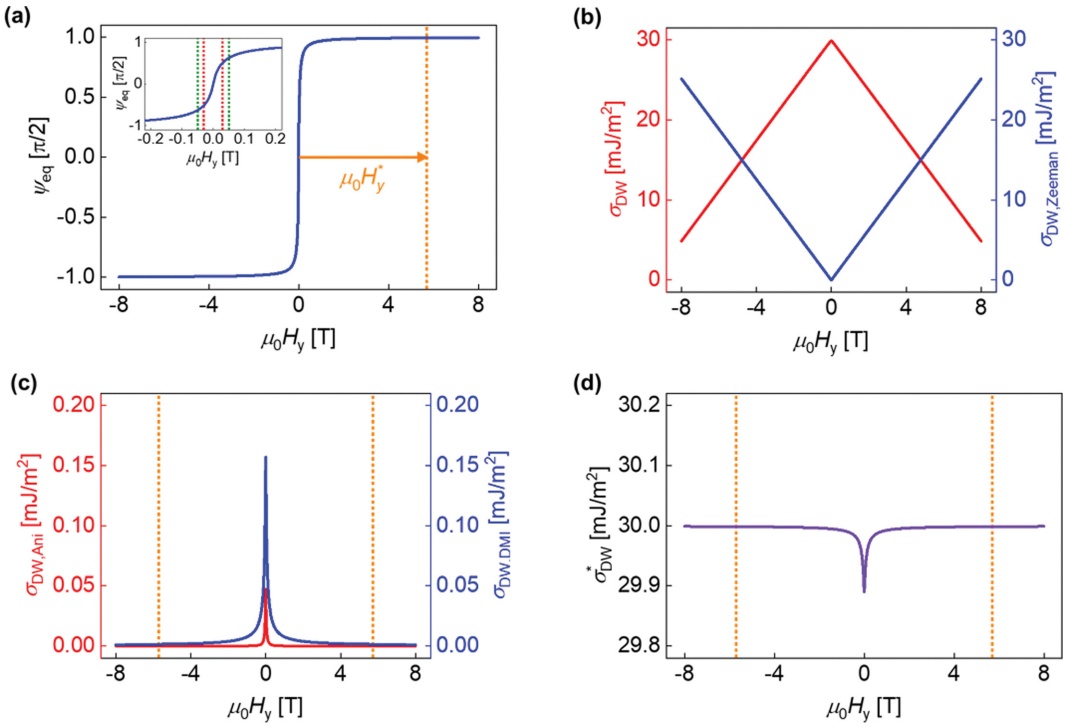


**Fig. 2.** (Color online) (a) Calculation of the equilibrium angle $\psi_{eq}$ as a function of in-plane magnetic field along y-direction $\mu_0H_y$. The parameters for this calculation are $\sigma_0$ = 30 mJ/m$^2$, $\mu_0H_S$ = 30 mT, $\lambda$ = 1 nm, $M_S$ = 1 MA/m, and $\mu_0H_{DMI}$ = 50 mT [31,38,40]. The orange arrow indicates the field that requires to achieve full Bloch-type configuration, called the critical field as $\mu_0H_y^*$. (b) Evolution of $\sigma_{DW}$ and $\sigma_{DW,Zeeman} \equiv \pi\lambda M_S\mu_0H_y\sin\psi_{eq}$ as a function of $\mu_0H_y$. (c) $\sigma_{DW,Ani} \equiv \pi\lambda K_D\cos^2\psi_{eq}$ and $\sigma_{DW,DMI} \equiv \pi\lambda M_S\mu_0H_{DMI}\cos\psi_{eq}$ as a function of $\mu_0H_y$. Orange dashed lines represents $|\mu_0H_y| = \mu_0H_y^*$. (d) Plot of the combined contribution of the Bloch-type DW energy density, anisotropy energy, and DMI-related term ($\sigma^*_{DW} \equiv \sigma_0 + \sigma_{DW,Ani} - \sigma_{DW,DMI}$) as a function of $\mu_0H_y$. Orange dashed lines represents $|\mu_0H_y| = \mu_0H_y^*$.

contribution, defined as $\sigma_{DW,Zeeman} \equiv \pi\lambda M_S \mu_0 H_y \sin\psi_{eq}$. This correspondence indicates that the Zeeman interaction primarily governs the overall reduction in DW energy. Additionally, we analyzed the DW anisotropy and DMI contributions, denoted as $\sigma_{DW,Ani} \equiv \pi\lambda K_D \cos^2\psi_{eq}$ and $\sigma_{DW,DMI} \equiv \pi\lambda M_S \mu_0 H_{DMI} \cos\psi_{eq}$ (Fig. 2(c)). As $\mu_0 H_y$ increases, $\sigma_{DW,Ani}$ gradually decreases, contributing to overall DW energy reduction. Conversely, $\sigma_{DW,DMI}$ tends to increase the total DW energy with increasing $\mu_0 H_y$. Notably, $\sigma_{DW,DMI}$ consistently exceeds $\sigma_{DW,Ani}$ throughout the examined field range, but eventually converges and matches $\sigma_{DW,Ani}$ at $|\mu_0 H_y| = \mu_0 H_y^*$ (orange dashed lines in Fig. 2(c)).

Fig. 2(d) plots the combined contribution of the Bloch-type DW energy density, anisotropy energy, and DMI-related term ($\sigma_{DW}^* \equiv \sigma_0 + \sigma_{DW,Ani} - \sigma_{DW,DMI}$) as a function of $\mu_0 H_y$. As previously noted, the DMI contribution continues to raise $\sigma_{DW}^*$ until $\mu_0 H_y$ approaches $\mu_0 H_y^*$ (orange dashed lines in Fig. 2(d)), where $\sigma_{DW,Ani}$ and $\sigma_{DW,DMI}$ become balanced. Beyond this point, $\sigma_{DW}^*$ saturates to a constant value, corresponding to the intrinsic Bloch-type DW energy density $\sigma_0$.

This behavior implies that mitigating the DMI-induced energy increase is essential for achieving $\psi_{eq} = \pm\pi/2$, suggesting a direct correlation between DMI magnitude and critical field $\mu_0 H_y^*$. Using the same parameters ($\sigma_0$ = 30 mJ/m$^2$, $\mu_0 H_S$ = 30 mT, $\lambda$ = 1 nm, and $M_S$ = 1 MA/m), we evaluated the dependence of $\mu_0 H_y^*$ on $\mu_0 H_{DMI}$, as shown in Fig. 3. The results affirm that the DMI-induced increase in DW energy critically determines $\mu_0 H_y^*$, leading to a substantially larger Néel-to-Bloch transition field. Despite the relatively small $\mu_0 H_{DMI}$ magnitude, aligning the DW magnetization along the y-axis requires an unexpectedly large external field, underscoring the strong resistance of the chiral DW configuration to transverse reorientation.

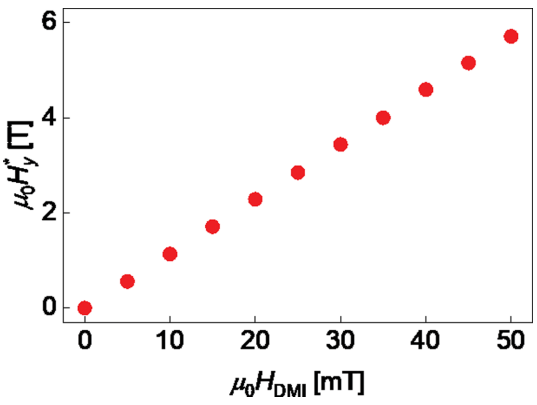


**Fig. 3.** (Color online) Plot of $\mu_0 H_y^*$ with resepct to $\mu_0 H_{DMI}$.

## III. Conclusion

In summary, this study uncovers distinct Zeeman energy contributions governing the Néel-to-Bloch transition based on the in-plane magnetic field orientation. When the external field is applied along the DW normal (longitudinal geometry), the DW anisotropy field primarily determines the transition. Conversely, when the field is applied along the DW plane (orthogonal geometry), the transition occurs at a much higher field than those dictated by DW anisotropy or DMI-induced fields. In both cases, increasing the field aligns the magnetization toward the field direction, reducing DW anisotropy and overall DW energy. However, the role of DMI differs in the longitudinal case, DMI acts as an effective shift field, reducing the total DW energy through its cooperative interaction with the Zeeman term. Conversely, in the orthogonal case, DMI competes with the Zeeman interaction, increasing DW energy as the magnetization deviates from the DW plane. This interplay between DMI and anisotropy explains the substantially larger Néel-to-Bloch transition field observed when the magnetic field is oriented along the DW plane. These findings uncover a hidden nonreciprocity in the field-driven energetics of chiral DWs, offering a novel approach to stabilize and manipulate DW chirality through directional magnetic-field control.

## Acknowledgements

We would like to thank Editage (www.editage.co.kr) for English language editing. This work was supported by the Korea Institute of Science and Technology (KIST) institutional program (grant 2E33581), and by the National Research Council of Science & Technology (NST) grant by the Korea government (MSIT) (No. GTL24041-000).

### Author Contributions

D.H.K. conceived the idea and supervised the research. J.Y. and D.H.K. developed the theoretical framework and analyzed the data. The manuscript was written by J.Y. and D.H.K. All authors participated in discussions of the results and reviewed of the manuscript.

### Additional information

Correspondence and requests for materials should be addressed to D.H.K.

### Competing financial interests

The authors declare no competing financial interests.

### Data availability

All data are available in the main text.

## References


[1] M. Bode, M. Heide, K. von Bergmann, P. Ferriani, S. Heinze, G. Bihlmayer, A. Kubetzka, O. Pietzsch, S. Blügel, and R. Wiesendanger, Nature **447**, 190 (2007).

[2] X. Z. Yu, Y. Onose, N. Kanazawa, J. H. Park, J. H. Han, Y. Matsui, N. Nagaosa, and Y. Tokura, Nature **465**, 901 (2010).

[3] A. Manchon, H. C. Koo, J. Nitta, S. M. Frolov, and R. A. Duine, Nat. Mater. **14**, 871 (2015).

[4] Y. Yoshimura, K.-J. Kim, T. Taniguchi, T. Tono, K. Ueda, R. Hiramatsu, T. Moriyama, K. Yamada, Y. Nakatani, and T. Ono, Nat. Phys. **12**, 157 (2016).

[5] G. Bihlmayer, P. Noël, D. V. Vyalikh, E. V. Chulkov, and A. Manchon, Nat. Rev. Phys. **4**, 642 (2022).

[6] S. S. P. Parkin, M. Hayashi, and L. Thomas, Science **320**, 190 (2008).

[7] J. H. Franken, H. J. M. Swagten, and B. Koopmans, Nat. Nanotech. **7**, 499 (2012).

[8] K.-S. Ryu, L. Thomas, S.-H. Yang, and S. Parkin, Nat. Nanotechnol. **8**, 527 (2013).

[9] O. Boulle, J. Vogel, H. Yang, S. Pizzini, D. d. S. Chaves, A. Locatelli, T. O. Menteş, A. Sala, L. D. Buda-Prejbeanu, O. Klein, M. Belmeguenai, Y. Roussigné, A. Stashkevich, S. M. Chérif, L. Aballe, M. Foerster, M. Chshiev, S. Auffret, I. M. Miron, and G. Gaudin, Nat. Nanotechnol. **11**, 449 (2016).

[10] K.-W. Moon, D.-H. Kim, S.-C. Yoo, S.-G. Je, B. S. Chun, W. Kim, B.-C. Min, C. Hwang, and S.-B. Choe, Sci. Rep. **5**, 9166 (2015).

[11] D.-H. Kim, D.-H. Kim, D.-Y. Kim, S.-B. Choe, T. Ono, K.-J. Lee, and S. K. Kim, Phys. Rev. B **102**, 184430 (2020).

[12] P. P. J. Haazen, E. Murè, J. H. Franken, R. Lavrijsen, H. J. M. Swagten, and B. Koopmans, Nat. Mater. **12**, 299 (2013).

[13] S. Emori, U. Bauer, S.-M. Ahn, E. Martinez, and G. S. D. Beach, Nat. Mater. **12**, 611 (2013).

[14] A. Thiaville, S. Rohart, É. Jué, V. Cros, and A. Fert, Europhys. Lett. **100**, 57002 (2012).

[15] E. Jué, C. K. Safeer, M. Drouard, A. Lopez, P. Balint, L. Buda-Prejbeanu, O. Boulle, S. Auffret, A. Schuhl, A. Manchon, I. M. Miron, and G. Gaudin, Nat. Mater. **15**, 272 (2016).

[16] Y. K. Kato, R. C. Myers, A. C. Gossard, and D. D. Awschalom, Science **306**, 1910 (2004).

[17] L. Liu, C.-F. Pai, Y. Li, H. W. Tseng, D. C. Ralph, and R. A. Buhrman, Science **336**, 555 (2012).

[18] I. M. Miron, G. Gaudin, S. Auffret, B. Rodmacq, A. Schuhl, S. Pizzini, J. Vogel, and P. Gambardella, Nat. Mater. **9**, 230 (2010).

[19] I. M. Miron, K. Garello, G. Gaudin, P.-J. Zermatten, M. V. Costache, S. Auffret, S. Bandiera, B. Rodmacq, A. Schuhl, and P. Gambardella, Nature **476**, 189 (2011).

[20] I. M. Miron, T. Moore, H. Szambolics, L. D. Buda-Prejbeanu, S. Auffret, B. Rodmacq, S. Pizzini, J. Vogel, M. Bonfim, A. Schuhl, and G. Gaudin, Nat. Mater. **10**, 419 (2011).

[21] J. Kim, J. Sinha, M. Hayashi, M. Yamanouchi, S. Fukami, T. Suzuki, S. Mitani, and H. Ohno, Nat. Mater. **12**, 240 (2013).

[22] D. Go, D. Jo, C. Kim, and H.-W. Lee, Phys. Rev. Lett. **121**, 086602 (2018).

[23] S. Lee, M.-G. Kang, D. Go, D. Kim, J.-H. Kang, T. Lee, G.-H. Lee, J. Kang, N. J. Lee, Y. Mokrousov, S. Kim, K.-J. Kim, K.-J. Lee, and B.-G. Park, Commun. Phys. **4**, 234 (2021).

[24] D. Lee, D. Go, H.-J. Park, W. Jeong, H.-W. Ko, D. Yun, D. Jo, S. Lee, G. Go, J. H. Oh, K.-J. Kim, B.-G. Park, B.-C. Min, H. C. Koo, H.-W. Lee, O. J. Lee, and K.-J. Lee, Nat. Commun. **12**, 6710 (2021).

[25] Y.-G. Choi, D. Jo, K.-H. Ko, D. Go, K.-H. Kim, H. G. Park, C. Kim, B.-C. Min, G.-M. Choi, and H.-W. Lee, Nature **619**, 52 (2023).

[26] I. E. Dzialoshinskii, Sov. Phys. JETP **5**, 1259 (1957).

[27] T. Moriya, Phys. Rev. **120**, 91 (1960).

[28] A. Fert and P. M. Levy, Phys. Rev. Lett. **44**, 1538 (1980).

[29] A. Fert, Mater. Sci. Forum **59-60**, 439 (1990).

[30] K.-W. Kim, H.-W. Lee, K.-J. Lee, and M. D. Stiles, Phys. Rev. Lett. **111**, 216601 (2013).

[31] S.-G. Je, D.-H. Kim, S.-C. Yoo, B.-C. Min, K.-J. Lee, and S.-B. Choe, Phys. Rev. B **88**, 214401 (2013).

[32] J. Cho, N.-H. Kim, S. Lee, J.-S. Kim, R. Lavrijsen, A. Solignac, Y. Yin, D.-S. Han, N. J. J. van Hoof, H. J. M. Swagten, B. Koopmans, and C.-Y. You, Nat. Commun. **6**, 7635 (2015).

[33] H. T. Nembach, J. M. Shaw, M. Weiler, E. Jué, and T. J. Silva, Nat. Phys. **11**, 825 (2015).

[34] D.-H. Kim, D.-Y. Kim, S.-C. Yoo, B.-C. Min, and S.-B. Choe, Phys. Rev. B **99**, 134401 (2019).

[35] D.-H. Kim, M. Haruta, H.-W. Ko, G. Go, H.-J. Park, T. Nishimura, D.-Y. Kim, T. Okuno, Y. Hirata, Y. Futakawa, H. Yoshikawa, W. Ham, S. Kim, H. Kurata, A. Tsukamoto, Y. Shiota, T. Moriyama, S.-B. Choe, K.-J. Lee, and T. Ono, Nat. Mater. **18**, 685 (2019).

[36] R. O'Handley, Modern Magnetic Materials: Principles and Applications, Wiley-Interscience, New York (2000) pp. 274-312.

[37] D.-Y. Kim, D.-H. Kim, J. Moon, and S.-B. Choe, Appl. Phys. Lett. **106**, 262403 (2015).

[38] D.-Y. Kim, D.-H. Kim, and S.-B. Choe, Appl. Phys. Express **9**, 053001 (2016).

[39] M. Kim and D.-H. Kim, Phys. Rev. B **112**, 024414 (2025).

[40] A. Hrabec, N. A. Porter, A. Wells, M. J. Benitez, G. Burnell, S. McVitie, D. McGrouther, T. A. Moore, and C. H. Marrows, Phys. Rev. B **90**, 020402(R) (2014).